BIOCHEMISTRY
including biophysical chemistry & molecular biology

Article

pubs.acs.org/biochemistry

Reaction of Human Cd_7metallothionein and *N*-Ethylmaleimide: Kinetic and Structural Insights from Electrospray Ionization Mass Spectrometry

Shu-Hua Chen and David H. Russell*

Department of Chemistry, Texas A&M University, College Station, Texas 77843, United States

Supporting Information

ABSTRACT: The reaction of cadmium-binding human metallothionein-2A (Cd_7MT) and *N*-ethylmaleimide (NEM) is investigated by electrospray ionization-ion mobility-mass spectrometry (ESI IM-MS). MS provides a direct measure of the distribution of the kinetic intermediates as the reaction proceeds and provides new insights into the relative kinetic stability of the individual metal−thiolate bonds in Cd_7MT. The rate constants for the various metal-retaining intermediates (Cd_i, intermediate with i Cd^{2+} ions attached) differ by >3 orders of magnitude: $Cd_4 \ll Cd_3 < Cd_2 < Cd_1 \sim Cd_6 < Cd_7 < Cd_5$. The reaction is viewed as a two-component cooperative process, rapid loss of three Cd^{2+} ions followed by slow loss of the remaining four Cd^{2+} ions, and $Cd_4NEM_{10}MT$ was observed as the least reactive intermediate during the entire displacement process. "MS-CID-IM-MS", a top-down approach that provides two-dimensional dispersion (size to charge by IM; mass to charge by MS) of the CID fragment ions, was used for direct analysis of the kinetic intermediate $[Cd_4NEM_{10}MT]^{5+}$ ion. The results provide direct evidence that the four Cd^{2+} ions located in the α-domain are retained, indicative of the greater kinetic stability for the α-domain. Further, the mapping of the alkylation sites in the $[Cd_4NEM_{10}MT]^{5+}$ ion reveals that not only the nine cysteines in the β-domain but Cys33 in the α-domain is selectively labeled. The kinetic lability of the Cd−Cys33 bond is unexpected. The structural and functional implications of these findings are discussed.

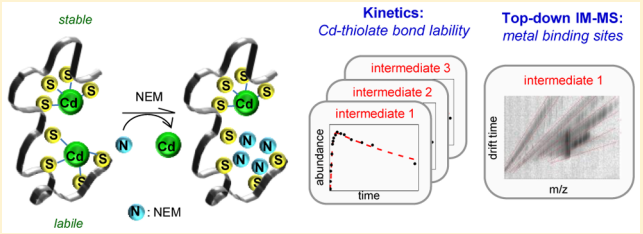

Metallothioneins (MTs) constitute a family of low-molecular weight proteins with a high cysteine and metal content.[1] MTs have the unusual ability to interact with a wide variety of metal ions through the formation of metal−thiolate bonds.[2,3] Human MTs are known to bind seven divalent (Cd^{2+} or Zn^{2+}) ions and form two metal−sulfur domains: a $(metal)_3(Cys)_9$ cluster in the N-terminal β-domain and a $(metal)_4(Cys)_{11}$ cluster in the C-terminal α-domain.[4−6] Although their exact function is not yet completely understood, they are known to play roles in the detoxification of heavy metal ions and regulation of essential metal ions.[2,3]

MTs have unique metal ion binding properties where the metal−sulfur bonds are highly thermodynamically stable and highly kinetically labile;[5,7,8] i.e., the metal−thiolate bonds undergo continuous breaking and re-forming within the metal clusters. The inherent kinetic lability of the metal−thiolate bonds and nucleophilicity of the thiolate sulfurs account for fundamental chemical processes of MTs,[9] including interprotein metal exchange/transfer and reactions with various oxidants and electrophiles.[9] The reactions with the non-metal electrophiles and oxidants *in vivo* are considered to offer protection against the deleterious effects of these toxic species.[10] Specifically, Kelly et al.[11] and Naganuma et al.[12] suggested that MTs confer resistance toward anticancer therapeutics by alkylation of the cysteine residues, which attenuates the toxicity of the antitumor therapeutics and provides intracellular drug sequestration.

The kinetic lability of the metal−thiolate bonds in MTs has been investigated by using metal-chelating ligands[13,14] and thiol-reactive electrophiles.[15−17] These competitive reactions were followed by monitoring the residual amount of bound metal ions using the absorbance of the metal−thiolate bonds or detecting the release of metal ions using metal-chelating fluorescent dyes. Results from these studies suggest that the reactions are biphasic with fast and slow steps, and it has been hypothesized that the two distinct phases arise from the independent reactions of the two metal−thiolate clusters.[13,14,16] However, the information derived from these spectroscopic measurements is limited to the metal ion flux; mechanistic details regarding the distribution of reaction intermediates over the course of the reactions and specific location(s) of the remaining metal ions bound in the reaction intermediates remain unclear. The major difficulty in characterizing the reaction intermediates lies in the fact that these intermediates are oftentimes heterogeneous in terms of the metal content and/or the extent of alkylation. The signal measured from these spectroscopic methods represents the sum of the responses for

Received: May 19, 2015
Revised: September 16, 2015
Published: September 16, 2015

DOI: 10.1021/acs.biochem.5b00545
Biochemistry 2015, 54, 6021−6028

all species in the reaction mixture; spectral features for a particular reaction intermediate can be masked in the total signal, resulting in a significant challenge in the interpretation of the spectroscopic data. It has not been possible to purify the individual components from the complex mixture for structural characterization.

On the other hand, using state-of-the-art MS-based techniques, it is possible to resolve the signals of the individual components[18−26] and to provide information regarding the metal-binding sites for a particular intermediate.[27−29] We have previously developed a MS-based methodology that identifies the relative kinetic stability (lability) of individual metal−thiolate bonds in the zinc finger domain of metal-response element-binding transcription factor-1 (MTF-1) and in *Staphylococcus aureas* plasmid pI258-encoded CadC using sulfhydryl-specific alkylating reagent *N*-ethylmaleimide (NEM).[30,31] The reaction of NEM and a thiol is a Michael type addition and is known to generate a covalent thioether bond.[32,33] The underlying principle of these studies relies on the fact that a metal-coordinated thiolate is a weaker nucleophile relative to a free thiolate;[34] viz., the reactivity of a thiolate is quenched when it is bound to a metal ion and is restored when dissociated, and the dynamic dissociative equilibrium of a metal−thiolate bond provides a "free" thiolate site for the rapid electrophilic attack by NEM. In this context, the rate of alkylation becomes a direct reporter for the intrinsic kinetic stability of a metal−thiolate bond.[30,31] Similar strategies have been used to distinguish states of the cysteine ligands (reduced or metal-bound) in MTs.[35−37] Recently, Stillman et al. used a cysteine labeling reagent to study conformations of the apo-α-domain fragment of human MT-1a.[38]

More recently, we developed a novel method that combines cysteine labeling, top-down proteomic strategy, and ion mobility mass spectrometry (IM-MS), a method using "MS-CID-IM-MS",[39] to directly determine the location of the metal ions in a partially metalated intermediate of human metallothionein-2A (MT) without the need for further sample preparation such as protein purification or enzymatic digestion.[29] In this experiment, ions of the partially metalated intermediate were m/z-selected by a quadrupole analyzer and then dissociated using collision-induced dissociation (CID). The CID product ions are then separated on the basis of size-to-charge ratio by the traveling-wave ion mobility separator and on the basis of m/z by the TOF mass analyzer. We have demonstrated that this two-dimensional separation effectively increases peak capacity, facilitating the direct assignment of the metal locations in the partially metalated MT.[29] Here we employ our methodologies to probe the kinetic lability of the dynamic metal−thiolate bonds in cadmium-saturated human metallothionein-2A (Cd_7MT) using cysteine alkylation and MS-CID-IM-MS. Information about chemical transformations of MT, the molecular distribution of reaction intermediates, and locations of metal ions and alkylation sites over the course of the reaction can be provided by MS, providing mechanistic insight into the metal displacement reaction and the kinetic stability of the metal−thiolate bonds in Cd_7MT.

MATERIALS AND METHODS

Sample Preparation. A cadmium-saturated MT-2A (Cd_7MT) powder sample (Bestenbalt LLC, Tallinn, Estonia; purity of >95%) was reconstituted to a concentration of 10 μM in 50 mM ammonium acetate buffer (pH 7.4) containing 10% methanol. The addition of 10% methanol in ESI enhances the signal-to-noise ratio without affecting the complexation of MT with metal ions.[19,40] The protein sequence is MDPNCSCAAG DSCTCAGSCK CKECKCTSCK KSCCSCCPVG CAKCAQ-GCIC KGASDKCSCC A. The ESI of the Cd_7MT solution (pH 7.4) yields 3+ to 5+ charge states with the 4+ charge state being most abundant, in line with the previous ESI data published by the Fenselau group.[18] The observed m/z value of the 4+ ion is 1704.8, which corresponds well with the expected value for the theoretical mass (6814.98 Da). The stability of the Cd_7MT solution was evaluated; protein oxidation and consequent metal loss were not observed under ambient conditions (25 °C, 1 atm) over a 24 h period. Displacement of the metal ions was performed by adding 1, 20, 40, 80, 200, 320, and 2000 equiv of NEM to a 10 μM Cd_7MT solution, resulting in solutions that contain 0.01, 0.2, 0.4, 0.8, 2.0, 3.2, and 20 mM NEM, respectively. The solutions were incubated for 1 h at 25 °C before being analyzed by ESI-MS. The kinetic study of the metal displacement reaction was conducted by adding 200 equiv of NEM to a 10 μM Cd_7MT solution. Aliquots were taken at various intervals from the time of mixing, and the reaction was monitored continuously by ESI-MS for 24 h at 25 °C.

To identify the metal ion-binding sites in a partially alkylated metal-retaining intermediate, the intermediate is m/z-selected and then subjected to the direct top-down sequencing; viz., a stable reaction intermediate Cd_4NEM_{10}MT obtained after a 1 h reaction of Cd_7MT and 200 equiv of NEM is directly analyzed by the MS-CID-IM-MS approach as described previously.[29]

Ion Mobility-Mass Spectrometry. All drift time and mass spectra were collected using a Waters (Manchester, U.K.) Synapt G2 HDMS instrument. A 10 μM sample solution was directly infused into the mass spectrometer at a flow rate of 0.5 μL/min. ESI spectra were collected in positive ion mode with a capillary voltage of 1.0−1.5 kV, a sample cone voltage of 10 V, and an extraction cone voltage of 1 V. The analysis of intact proteins was conducted under conditions that minimize ion heating.[41] All mass spectra were calibrated externally using a solution of sodium iodide. A TW wave velocity of 300 m/s and a wave height of 20 V were used. N_2 flow in the traveling wave ion mobility cell was maintained at 2.98 mbar.

Kinetic Analysis. Perez-Rafael et al. showed that ESI signals of metal−MT species that differ in the degree of metalation can be related to their relative abundances in solution.[25] Kurono et al. concluded that ionization efficiencies of peptides do not appear to be significantly influenced by NEM modification.[42] Thus, the various MT species can be thought to have similar ionization efficiencies in this study. The abundance of each ion was determined by performing a baseline correction and calculating the area under the peak. To simplify the kinetic analysis, $Cd_iNEM_xMT^{n+}$ ions that have the same number of metal ions bound (i) but differ in the degree of alkylation (x) and charge state (n) were summed together to provide a total abundance of the Cd_i species. The amounts of bound metal ion in the protein and free NEM in solution over the course of the reaction were estimated from the abundances of the metal-displaced Cd_i products (see mass-balanced eqs 1 and 2). An average stoichiometry (s) of bound NEM to displaced Cd^{2+} is used to simplify the calculation of NEM concentration. The s is assumed to be 2.86, which is calculated by dividing 20 NEM by 7 Cd^{2+} in the case of Cd_7MT.

DOI: 10.1021/acs.biochem.5b00545
Biochemistry 2015, 54, 6021−6028

$$[Cd^{2+}]_{bound,t} = [Cd^{2+}]_{bound,0} - [Cd_6]_t - 2[Cd_5]_t - 3[Cd_4]_t - 4[Cd_3]_t - 5[Cd_2]_t - 6[Cd_1]_t - 7[Cd_0]_t \quad (1)$$

$$[NEM]_{free,t} = [NEM]_{free,0} - s[Cd_6]_t - 2s[Cd_5]_t - 3s[Cd_4]_t - 4s[Cd_3]_t - 5s[Cd_2]_t - 6s[Cd_1]_t - 7s[Cd_0]_t \quad (2)$$

The kinetic data were analyzed using Mathematica (Wolfram Research Inc., Champaign, IL). A seven-step reaction model was proposed to account for the reaction of Cd_7MT and NEM (eq 3). Each step of the reaction is proposed to follow second-order kinetics with respect to $[Cd_i]_t$ and $[NEM]_t$. A retro-Michael reaction that reverses a thioether back to the starting thiol and maleimide has been proposed;[15,33] however, in the absence of excess free thiols, the thioether bonds are generally considered stable.[33] The detailed rate laws and boundary conditions are provided in the Supporting Information. The seven rate constants were obtained by fitting the numerical solution of the rate equations to the experimental data using Mathematica.

$$Cd_7 \xrightarrow[NEM]{k_7} Cd_6 \xrightarrow[NEM]{k_6} Cd_5 \xrightarrow[NEM]{k_5} Cd_4 \xrightarrow[NEM]{k_4} Cd_3 \xrightarrow[NEM]{k_3} Cd_2 \xrightarrow[NEM]{k_2} Cd_1 \xrightarrow[NEM]{k_1} Cd_0 \quad (3)$$

RESULTS

Figure 1 includes the MS spectra of cases in which the alkylation reagent NEM was added to displace the metal ions from Cd_7MT. The addition of NEM is detected by MS with a mass shift of +125.04 Da. The data show that the reaction proceeds via alkylation of the fully metalated form and finally results in concomitant metal loss. For example, the addition of small amounts of NEM (<40 equiv) does not lead to a significant amount of Cd^{2+} displacement. Note that the fully metalated Cd_7MT is found to react with a small number of NEMs before losing the metal ions; e.g., Cd_7NEM_3MT is present at 20 equiv of NEM (Figure 1). Increasing the concentration of NEM yields more extensive NEM labeling and subsequent metal release. Following addition of 40 equiv of NEM, product ions corresponding to four Cd^{2+}-bound metalated intermediates (abbreviated as Cd_4 species) were observed. If one starts from the Cd_4 species, there is a marked lowering of the reactivity toward further alkylation. Above 80 equiv of NEM, the $Cd_4NEM_{10}MT$ intermediate is the most abundant product. In the solutions having a large molar excess of NEM (2000:1 NEM:Cd_7MT), the $Cd_4NEM_{10}MT$ remains as the dominant species and the metal-stripped MT ($NEM_{20}MT$) is also detected in low abundance.

The reaction intermediate $Cd_4NEM_{10}MT$ was directly analyzed by MS-CID-IM-MS[29] to identify the locations of metal ions and NEMs. For example, $[Cd_4NEM_{10}MT]^{5+}$ ions were m/z-selected prior to CID and the fragment ions generated by CID were analyzed by ion mobility and mass analyzers. The two-dimensional (2D) IM-MS plot for the CID product ions is shown in Figure S1 of the Supporting Information. The data show that ions that have different properties (charge and metalated states) are dispersed along different trendlines. The trendline-specific mass spectra are shown in Figure 2A. The β-domain fragment ions (b ions, b_2–NEM_7b_{25}; y ions, $Cd_4NEM_1y_{31}$–$Cd_4NEM_{10}y_{60}$) suggest that the nine cysteines in the β-domain are labeled by NEM. The α-domain fragment ions (Cd_2y_5–$Cd_4NEM_1y_{30}$) also provide evidence that the four Cd^{2+} ions are located in the α-domain. In addition, the presence of fragment ions Cd_4y_{28} and $Cd_4NEM_1y_{29}$ is consistent with alkylation of Cys33 in the α-domain. This result is consistent with the differential sulfur reactivity of the domains; i.e., the three Cd^{2+} ions in the β-domain are relatively labile, and thus, the corresponding metal–thiolate bonds are prone to react with NEM whereas the four Cd^{2+} ions residing in the α-domain are strongly bound even in the presence of a high concentration of NEM. It is noted that although NEM could potentially react with amino acids other than cysteines, evidence for such reactions is not observed under the conditions used here.

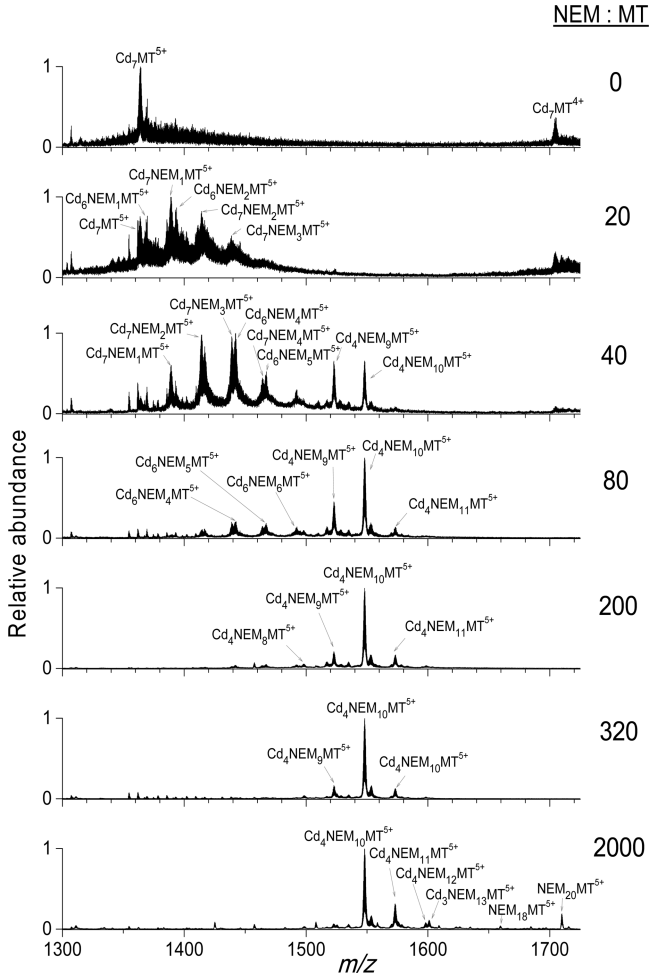

Figure 1. ESI-MS spectra of Cd_7MT solutions (pH 7.4) to which 1–2000 equiv NEM had been added. The spectra were taken after incubation at 25 °C for 1 h. The $Cd_4NEM_{10}MT$ ion was observed as the most stable intermediate during the displacement reactions. Data shown limited to the 5+ region.

The kinetics of the metal displacement reaction was investigated by monitoring the individual signals as a function of time while the NEM concentration is held constant (200:1 NEM:Cd_7MT) (see Figure S2 of the Supporting Information for the detailed MS spectra). As expected, the reaction occurred through sequential displacement of metal ions and multiple partially alkylated metal-retaining intermediates Cd_iNEM_xMT (i = 6–1; x = 0–19) were sequentially formed. It should be

DOI: 10.1021/acs.biochem.5b00545
Biochemistry 2015, 54, 6021–6028

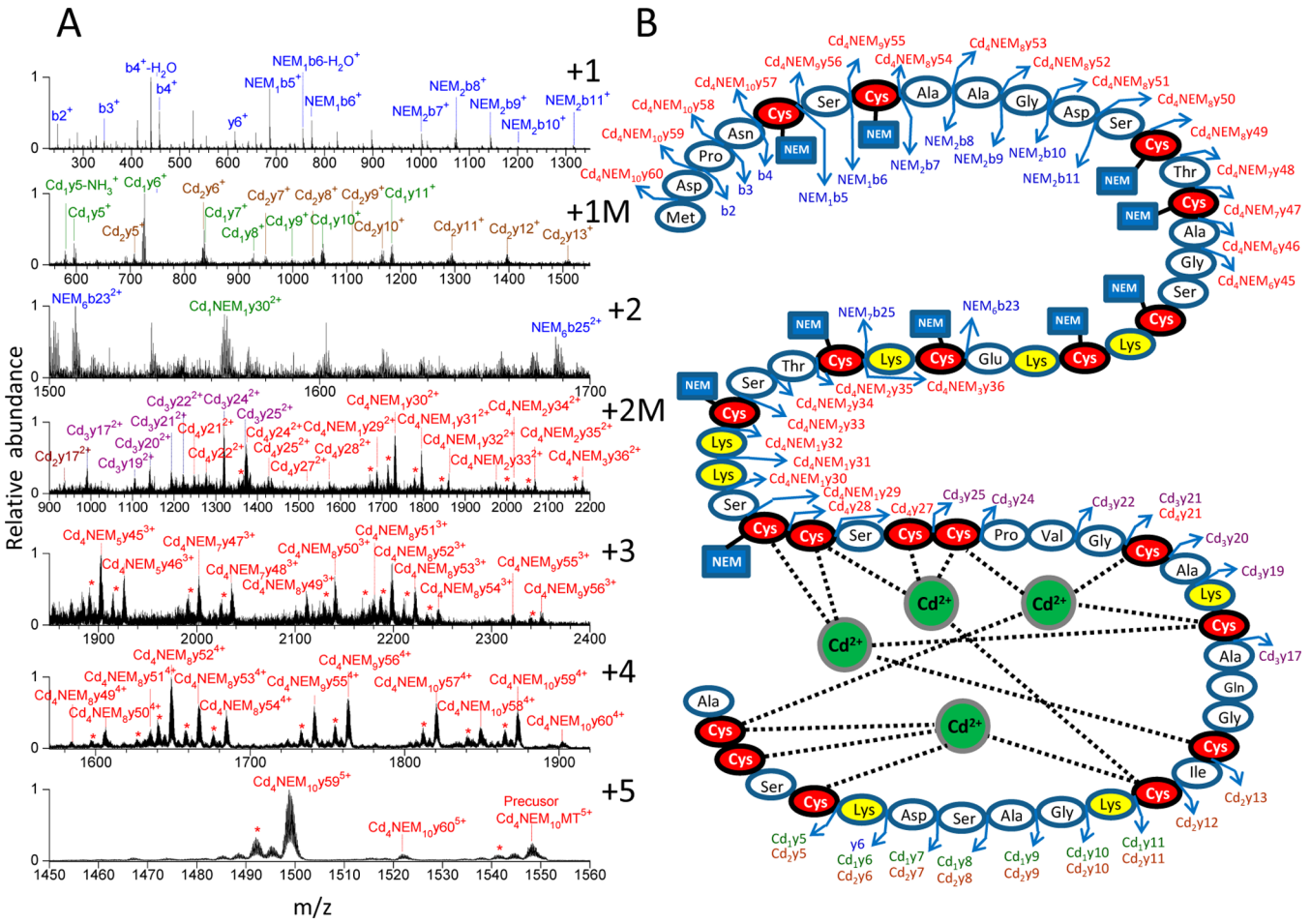

Figure 2. MS-CID-IM-MS analysis of the partially alkylated metal-retaining intermediate $[Cd_4NEM_{10}MT]^{5+}$. The ion was produced after a 1 h reaction of Cd_7MT and 200 equiv of NEM (pH 7.4) at 25 °C as described in Figure 1. (A) Trendline-specific mass spectra extracted from the 2D MS-CID-IM-MS plot (see Figure S1 of the Supporting Information). Peaks with an asterisk are ions that are shifted by ~ 35 Da from the y fragment ions, corresponding to loss of ammonia and water. (B) Summary of the identified fragment ions and the corresponding model. This result provides direct evidence that the four Cd^{2+} ions located in the α-domain are retained in the displacement reaction. We note that the cadmium−thiolate coordination geometry shown in panel B is adapted from the previous NMR human Cd_7MT-2A study[4] and may rearrange in the case of $Cd_4NEM_{10}MT$.

noted that different NEM concentrations were tested; 200 equiv of NEM provided the best reaction time scale for detection of all the intermediates by MS.

Figure 3 contains kinetic plots for the individual Cd_i intermediates and end product Cd_0. The starting material Cd_7 appears to follow an exponential decay, and the reaction intermediates Cd_6−Cd_1 sequentially rise and decay with time until the final product Cd_0 is formed. Changes in the free NEM concentration (Figure 3I) as well as the equivalents of Cd^{2+} ions retained by MT (Figure 3J) over the course of the reaction can be estimated from the abundances of the metal-displaced Cd_i products (see Materials and Methods). A biexponential decay is observed for the bound Cd^{2+} with a cross point at 1.4 that corresponds to 4.3 equiv of Cd^{2+} (Figure 3J). These data suggest that the release of the first three metal ions was fast ($k_{Cd^{2+},fast}$ = 8.4 × 10^{-3} min^{-1}; <50 min), but removal of the last four metal ions required >24 h ($k_{Cd^{2+},slow}$ = 4.8 × 10^{-4} min^{-1}). Although we found that the concentration of free NEM does not change significantly over the 24 h reaction period (Figure 3I; the change in NEM concentration is <7.5%), to more accurately describe the kinetics of the chemical reaction, seven sequential second-order reactions with respect to the concentrations of Cd_i and NEM were constructed (see the Supporting Information for the detailed rate laws).

The kinetic data for the individual Cd_i reveal four classes of reaction rates that differ by >3 orders of magnitude: (i) 10^{-1} M^{-1} min^{-1}, k_4; (ii) 10^{0} M^{-1} min^{-1}, k_3; (iii) 10^{1} M^{-1} min^{-1}, k_2, k_1, k_6, and k_7; (iv) 10^{2} M^{-1} min^{-1}, k_5. For the displacement of metal ions in the first step (Cd_7−Cd_4), the rates of dissociation of the first and second metal ions (k_7 and k_6, respectively) are moderate (~10^{1} M^{-1} min^{-1}) while the third metal ion is lost much faster [16-fold; k_5 = 450 M^{-1} min^{-1} (Figure 3C)]. A similar kinetic pattern was observed for the displacement of metal ions in the second step (Cd_4−Cd_0). The metal displacement of the Cd_4 species was very slow [k_4 = 0.26 M^{-1} min^{-1} (Figure 3D)], while the rates of the loss of the remaining three Cd^{2+} ions were much faster (Figure 3E, 13-fold for the fifth metal ion, k_3 = 3.4 M^{-1} min^{-1}; Figure 3F, 50-fold for the sixth metal ion, k_2 = 13 M^{-1} min^{-1}; Figure 3G, 96-fold for the seventh metal ion, k_1 = 25 M^{-1} min^{-1}).

DISCUSSION

Thiol chemistry is known as the central aspect to MT's mechanism of action and biological function.[3] Specifically, the

DOI: 10.1021/acs.biochem.5b00545
Biochemistry 2015, 54, 6021−6028

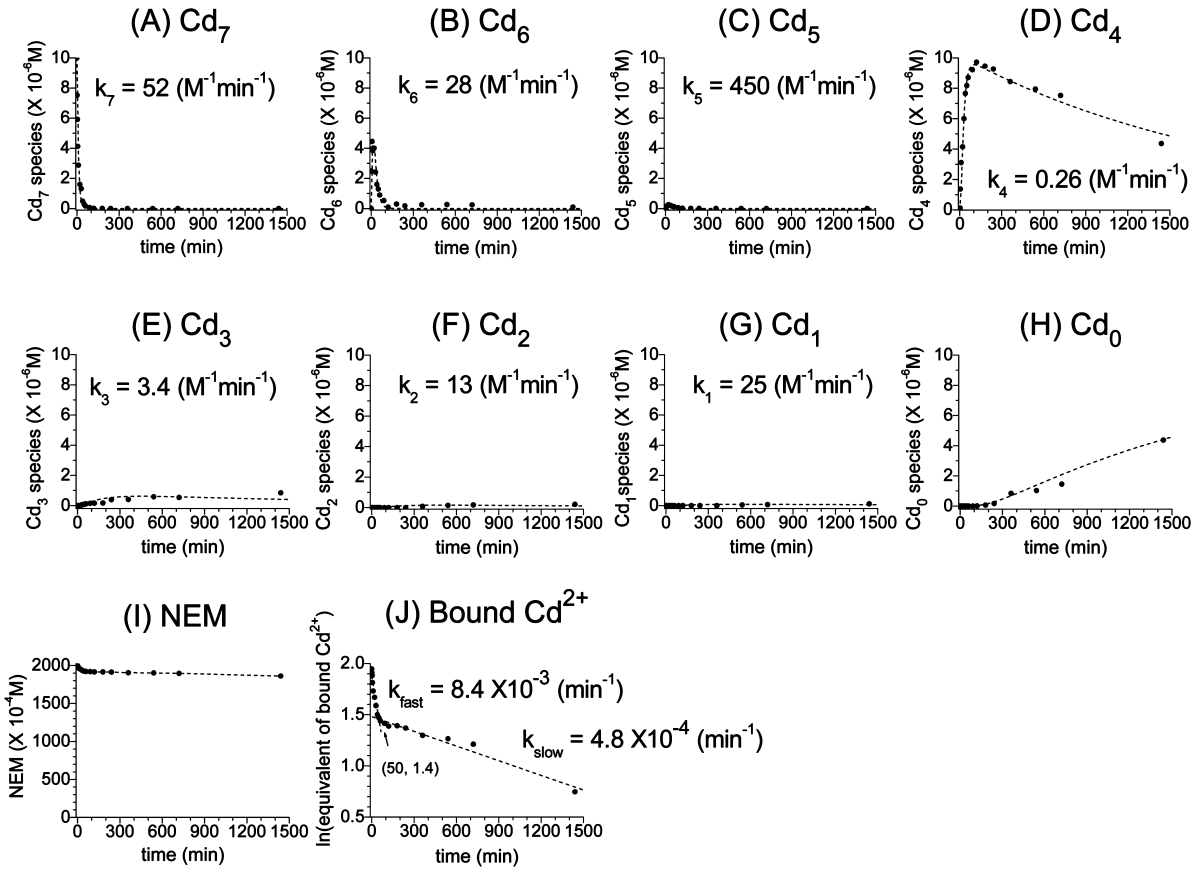

Figure 3. Kinetic plots for the individual Cd_i species (i = 0−7). The reaction was conducted by adding 200 equiv of NEM to a solution of 10 μM Cd_7MT (pH 7.4). The reaction was continuously monitored by ESI-MS over 24 h at 25 °C. The signals for $Cd_iNEM_xMT^{n+}$ that have the same number of metal ions bound (i) but differ in the number of NEMs (x) and charge state (n) are summed together to provide a total abundance of the Cd_i species. The data points are the observed abundances, and the dashed lines are fitting curves. The rate constants are obtained by fitting the numerical solution of the rate equations to the experimental data (see Materials and Methods). We note that this kinetics experiment is repeated several times and very consistent results were obtained; a single data set was thus chosen to illustrate representative data.

chemical reactivity of fully metalated MTs is determined by the kinetic lability of the metal−thiolate bonds and the nucleophilicity of the thiolate sulfurs.[9] It has been shown that the two metal−thiolate clusters differ significantly in (1) metal ion binding properties, (2) cysteine sulfur reactivities, and (3) potentials to donate the metal ions to an apo-metalloprotein.[6,13,14,16,27,28,36,43] In the demetalation or metal displacement reactions of $(metal)_7$MT, the observation that the metal ions are released via a biphasic kinetic pattern has led to the suggestion that the metal−thiolate interaction in one of the two clusters is more labile than the other;[13,14,16] which of the two clusters is more reactive was assigned by comparison of the reaction rates of intact protein to that of isolated domains.[14,16] However, it is well-documented that domain−domain interactions play roles in intact MT's reactivity and structure, and properties of the individual domains do not suffice to describe the intact MT either structurally or functionally.[43,44] This suggests that the presence of the other domain may influence the reactivity of the domain under study, and results obtained from the isolated domains may not be comparable to the way they function together in the intact protein.[45]

Here, the relative stability (lability) of the metal−thiolate bonds in intact Cd_7MT was directly probed using cysteine alkylation and top-down MS. The rate of thiolate alkylation is used to indicate the stability of the metal−thiolate bonds; the MS-based detection provides a means for direct structural access to a particular intermediate in the progression of the reaction.

The topology for the stable reaction intermediate $Cd_4NEM_{10}MT$ contained in Figure 2B provides unambiguous evidence that metal−thiolate bonds in the two domains display vastly different reactivities toward the alkylating reagent NEM. The cysteinyl sulfurs in the β-domain are selectively targeted by NEM, consistent with the greater kinetic lability of the metal−thiolate bonds in the β-domain. The data also suggest that the metal−thiolate coordination in the α-domain is relatively tight, which results in substantial protection against the alkylation. This result correlates well with the high thermodynamic stability of the α-domain and the more rapid metal ion exchange of the β-domain observed by NMR.[46]

Additionally, the seemingly two-step reaction described by the spectroscopic studies can be dissected into the multistep kinetics by our MS-based strategy. The new information revealed here is the chemical transformation of Cd_7MT to the various Cd_i intermediates over time. The rate constants contain information about the mechanisms of the displacement reaction and the metal binding properties of MT. Figure 3 shows distinct rate constants of these intermediates that differ by >3 orders of magnitude, in the following order: $Cd_4 \ll Cd_3 < Cd_2 < Cd_1 \sim Cd_6 < Cd_7 < Cd_5$. We interpret this data as follows. (i) The metal dissociation rates in the α-domain (k_4−k_1) are much

DOI: 10.1021/acs.biochem.5b00545
Biochemistry 2015, 54, 6021−6028

slower than that in the β-domain (k_7–k_5), indicating stronger metal–thiolate coordination and greater kinetic stability of the α-domain. (ii) The releases of the second metal ion (Cd_6 = 28 M^{-1} min^{-1}) and the fourth metal ion (Cd_4 = 0.26 M^{-1} min^{-1}) are rate-determining steps for the β-domain and the α-domain that account for the well-known biphasic kinetic profile observed using the spectroscopic measurments;[15] however, the slight difference between k_7 (52 M^{-1} min^{-1}) and k_6 (28 M^{-1} min^{-1}) is difficult to probe by other methods. (iii) k_7 is faster than k_6, suggesting that there is a weakly bound Cd^{2+} in the β-domain, in line with the previous observation made by Kagi et al.[36,47] The data show that reasonable fits were obtained, although it should be noted that the reaction might be more complicated than the second-order kinetic model we proposed here. It should also be noted that the fitting parameter $[NEM]_t$ is approximated on the basis of the average replacement stoichiometry that may introduce errors in the fitting of rate constants. Errors in determining the ion abundances from the raw mass spectra (especially for intermediates that have a lower signal-to-noise ratio such as Cd_i, i = 5, 2, and 1) may also result in less satisfactory fits.

It has been proposed that the metal binding in each domain of MT is cooperative.[13,19,20,48] The evidence for this is the observation of a preferentially formed intermediate associated with both metalation and demetalation processes, viz., Cd_4MT. Recently, however, Stillman et al. proposed a noncooperative binding model based on the observation of a sequential, independent metal binding manner in the metalation process.[49] The inconsistency between these studies could arise from different protein isoforms and/or different metal ions used in the studies as there is growing awareness that the metal binding properties of one isoform cannot be directly applied to that of other isoforms.[2,50] The discrepancy could also arise from slightly different experimental conditions such solvent composition and pH.[19] It should be noted that sample oxidation and ion heating may occur during the ESI sampling process,[29,41] which could potentially alter the reaction products and mislead the interpretation of data. The kinetic plots contained in Figure 3 clearly show a cooperative loss of Cd^{2+} ions for each domain in the metal displacement reaction; viz., the rates of metal dissociation in the β-domain were $Cd_7 \sim Cd_6 < Cd_5$ and in the α-domain $Cd_4 \ll Cd_3 < Cd_2 < Cd_1$. It is noted that the oxidative alkylation reaction studied here is different from the metalation/demetalation reaction. Whether a reaction is cooperative may well depend on the type of reaction, and each reaction needs to be examined independently.

Previous studies of demetalation of fully metalated MTs (Cd_7MT and Zn_7MT) using ethylenediaminetetraacetic acid (EDTA) have established that the three metal ions in the β-domain are more labile than the four metal ions in the α-domain.[13,18] In spite of the success in following the metal ions flux, these studies do not provide "site-specific" information in terms of the kinetic lability of the cysteine positions. In this study, the labile thiolates are targeted by NEM, resulting in oxidative alkylation and subsequent loss of metal ion. Top-down MS was followed to directly read the reaction sites. The data contained in Figure 2 revealed that the α-domain-binding site Cys33 has a dual personality; i.e., it is located in the α-domain but behaves like the cysteines in the β-domain in terms of metal displacement reaction. Petering et al. showed that alkylation of rabbit liver MT by substoichiometric levels of NEM results in a complete loss of NMR signals for both metal–thiolate clusters.[15] The detailed alkylation map in our study may help explain and/or consolidate their observation. In addition, the labeling on Cys33 suggests that the binding strength of the four cysteinyl ligands to a single Cd^{2+} is not equal and Cys33 is weakly coordinated to the α metal–thiolate cluster. The relatively high stability of the $Cd_4NEM_{10}MT$ intermediate implies that the "capping" of the Cys33 does not lead to cooperative collapse of the α-domain. However, signals attributed to the intermediates that have additional NEM replacement in the α-domain (Cd_4NEM_xMT, where $x > 10$) are relatively small, indicating that any other cysteines in the α-domain may play more significant roles in stabilizing the α-domain cluster. This result also shows that the 10 cysteines are sufficient to hold the four α-domain Cd^{2+} ions, suggesting that the α-domain cluster may rearrange and a terminal cysteinyl ligand may become bridging to maintain the tetrahedral coordination of cadmium ions in the alkylation reaction.

The selective alkylation of Cys33 is intriguing as in fact it is expected to be engaged in the metal coordination of the α-domain cluster. Fenselau et al. also reported the specific reactivity of Cys33; i.e., Cys33 was one of the two sites that are selectively targeted by anticancer reagents.[27,28] In fact, the thiolate reactivity can be altered by its solvent accessibility and whether an intramolecular NH···S hydrogen bond is present.[27,51] Inspection of the crystal structure of rat Cd_5Zn_2MT suggests that the cysteine sulfur atoms vary greatly in their solvent accessibility.[5] For example, Cys33, -36, -41, and -59 in the α-domain and Cys7 and -13 in the β-domain are highly solvent exposed (>12 Å^2).[5] Thus, the observation of NEM alkylation on Cys33 may be attributed to its sulfur solvent accessibility. It is also important to note that the Cys33 is located in the cleft between the α- and β-domains, which may make it possible for this site to participate in the metal coordination in both domains. Huang et al. showed that monkey MT-1 loses the cooperative properties when the Cys33 is mutated.[52] Whether Cys33 plays a functional role in domain interaction requires further evaluation and is an aspect that we are currently investigating.

CONCLUSION

Reactions of MT usually proceed via a series of heterogeneous intermediates that differ in terms of structures and metal composition. MS provides a direct access to measure all the species in the reaction mixtures, thus allowing a more complete description of the processes. When combined with tandem mass spectrometric strategies, MS offers a unique opportunity to simultaneously study the distribution of the reaction intermediates, the progression of the reactions, and the structures of the partially metalated intermediates, thus complementing the information derived from the spectroscopic measurements. The strategy presented here utilizes the differential reactivity of the cysteine thiolates toward the electrophile NEM; the rate of NEM labeling is used to indicate the lability of the metal–thiolate bonds in Cd_7MT. The kinetic profiles for the intermediates provide direct mechanistic insights into the metal displacement reaction, and the data support the cooperative binding model for the domains. The direct MS-CID-IM-MS analysis of the reaction intermediate reveals that the thiolates in the β-domain and at Cys33 are kinetically labile, indicative of the dual personality of the Cys33 as well as the greater lability of the β-domain relative to that of the α-domain. On the other hand, the remaining α-domain cluster contains four Cd^{2+} ions and 10 cysteines, indicating that 10 cysteines are sufficient to hold the four α-domain Cd^{2+} ions

DOI: 10.1021/acs.biochem.5b00545
Biochemistry 2015, 54, 6021–6028

and the Cd−S coordination may rearrange to maintain the cluster in the alkylation reaction. The data also highlight the utility of ion mobility in providing increased ion separation that allows the direct identification of the modified sites. We anticipate that this approach will have wide applicability in other complex protein−multiligand systems.

■ ASSOCIATED CONTENT

Supporting Information

The Supporting Information is available free of charge on the ACS Publications website at DOI: 10.1021/acs.biochem.5b00545.

Detailed rate laws and boundary conditions of the kinetic model for the reaction of NEM and Cd_7MT, 2D IM-MS plot for the CID fragment ions of $[Cd_4NEM_{10}MT]^{5+}$, and time course for the displacement of Cd^{2+} ions from Cd_7MT by 200 equiv of NEM. (PDF)

■ AUTHOR INFORMATION

Corresponding Author

*E-mail: russell@chem.tamu.edu. Telephone: 979-845-3345. Fax: 979-845-9485.

Funding

We thank the Robert A. Welch Foundation (A-1176) for providing financial support for S.-H.C. and the U.S. Department of Energy, Division of Chemical Sciences, BES (DE-FG02-04R15520), for funding the fundamental IM-MS research.

Notes

The authors declare no competing financial interest.

■ ABBREVIATIONS

ESI, electrospray ionization; MS, mass spectrometry; IM, ion mobility; MT, metallothionein; CID, collision-induced dissociation; NEM, *N*-ethylmaleimide.

■ REFERENCES

(1) Margoshes, M., and Vallee, B. L. (1957) A cadmium protein from equine kidney cortex. *J. Am. Chem. Soc. 79*, 4813−4814.

(2) Blindauer, C. A., and Leszczyszyn, O. I. (2010) Metallothioneins: unparalleled diversity in structures and functions for metal ion homeostasis and more. *Nat. Prod. Rep. 27*, 720−741.

(3) Li, Y., and Maret, W. (2008) Human metallothionein metallomics. *J. Anal. At. Spectrom. 23*, 1055−1062.

(4) Messerle, B. A., Schaffer, A., Vasak, M., Kagi, J. H., and Wuthrich, K. (1990) Three-dimensional structure of human [$^{113}Cd_7$]-metallothionein-2 in solution determined by nuclear magnetic resonance spectroscopy. *J. Mol. Biol. 214*, 765−779.

(5) Robbins, A. H., McRee, D. E., Williamson, M., Collett, S. A., Xuong, N. H., Furey, W. F., Wang, B. C., and Stout, C. D. (1991) Refined crystal structure of Cd, Zn metallothionein at 2.0 A resolution. *J. Mol. Biol. 221*, 1269−1293.

(6) Romero-Isart, N., and Vasak, M. (2002) Advances in the structure and chemistry of metallothioneins. *J. Inorg. Biochem. 88*, 388−396.

(7) Vasak, M., Hawkes, G. E., Nicholson, J. K., and Sadler, P. J. (1985) 113Cd NMR studies of reconstituted seven-cadmium metallothionein: evidence for structural flexibility. *Biochemistry 24*, 740−747.

(8) Kagi, J. H., and Schaffer, A. (1988) Biochemistry of metallothionein. *Biochemistry 27*, 8509−8515.

(9) González-Duarte, P. (2003) Metallothioneins. In *Comprehensive Coordination Chemistry II* (Meyer, J. A. M. J., Ed.) pp 213−228, Pergamon, Oxford, U.K.

(10) Namdarghanbari, M., Wobig, W., Krezoski, S., Tabatabai, N. M., and Petering, D. H. (2011) Mammalian metallothionein in toxicology, cancer, and cancer chemotherapy. *JBIC, J. Biol. Inorg. Chem. 16*, 1087−1101.

(11) Kelley, S. L., Basu, A., Teicher, B. A., Hacker, M. P., Hamer, D. H., and Lazo, J. S. (1988) Overexpression of metallothionein confers resistance to anticancer drugs. *Science 241*, 1813−1815.

(12) Naganuma, A., Satoh, M., and Imura, N. (1987) Prevention of lethal and renal toxicity of cis-diamminedichloroplatinum(II) by induction of metallothionein synthesis without compromising its antitumor activity in mice. *Cancer Res. 47*, 983−987.

(13) Gan, T., Munoz, A., Shaw, C. F., 3rd, and Petering, D. H. (1995) Reaction of $^{111}Cd_7$-metallothionein with EDTA. A reappraisal. *J. Biol. Chem. 270*, 5339−5345.

(14) Li, H., and Otvos, J. D. (1998) Biphasic kinetics of Zn^{2+} removal from Zn metallothionein by nitrilotriacetate are associated with differential reactivity of the two metal clusters. *J. Inorg. Biochem. 70*, 187−194.

(15) Shaw, C. F., III, He, L., Muñoz, A., Savas, M. M., Chi, S., Fink, C. L., Gan, T., and Petering, D. H. (1997) Kinetics of reversible N-ethylmaleimide alkylation of metallothionein and the subsequent metal release. *JBIC, J. Biol. Inorg. Chem. 2*, 65−73.

(16) Savas, M. M., Petering, D. H., and Shaw, C. F. (1991) On the rapid, monophasic reaction of the rabbit liver metallothionein alpha-domain with 5,5′-dithiobis (2-nitrobenzoic acid) (DTNB). *Inorg. Chem. 30*, 581−583.

(17) Muñoz, A., Petering, D. H., and Shaw, C. F. (1999) Reactions of electrophilic reagents that target the thiolate groups of metallothionein clusters: Preferential reaction of the α-Domain with 5,5′-dithio-bis(2-nitrobenzoate) (DTNB) and aurothiomalate (AuSTm). *Inorg. Chem. 38*, 5655−5659.

(18) Zaia, J., Fabris, D., Wei, D., Karpel, R. L., and Fenselau, C. (1998) Monitoring metal ion flux in reactions of metallothionein and drug-modified metallothionein by electrospray mass spectrometry. *Protein Sci. 7*, 2398−2404.

(19) Gehrig, P. M., You, C., Dallinger, R., Gruber, C., Brouwer, M., Kagi, J. H., and Hunziker, P. E. (2000) Electrospray ionization mass spectrometry of zinc, cadmium, and copper metallothioneins: evidence for metal-binding cooperativity. *Protein Sci. 9*, 395−402.

(20) Meloni, G., Zovo, K., Kazantseva, J., Palumaa, P., and Vasak, M. (2006) Organization and assembly of metal-thiolate clusters in epithelium-specific metallothionein-4. *J. Biol. Chem. 281*, 14588−14595.

(21) Knipp, M., Karotki, A. V., Chesnov, S., Natile, G., Sadler, P. J., Brabec, V., and Vasak, M. (2007) Reaction of Zn7metallothionein with cis- and trans-[Pt(N-donor)2Cl2] anticancer complexes: trans-Pt(II) complexes retain their N-donor ligands. *J. Med. Chem. 50*, 4075−4086.

(22) Ngu, T. T., and Stillman, M. J. (2006) Arsenic binding to human metallothionein. *J. Am. Chem. Soc. 128*, 12473−12483.

(23) Ngu, T. T., Easton, A., and Stillman, M. J. (2008) Kinetic analysis of arsenic-metalation of human metallothionein: significance of the two-domain structure. *J. Am. Chem. Soc. 130*, 17016−17028.

(24) Palumaa, P., Eriste, E., Njunkova, O., Pokras, L., Jornvall, H., and Sillard, R. (2002) Brain-specific metallothionein-3 has higher metal-binding capacity than ubiquitous metallothioneins and binds metals noncooperatively. *Biochemistry 41*, 6158−6163.

(25) Perez-Rafael, S., Atrian, S., Capdevila, M., and Palacios, O. (2011) Differential ESI-MS behaviour of highly similar metallothioneins. *Talanta 83*, 1057−1061.

(26) Chen, S.-H., Chen, L., and Russell, D. H. (2014) Metal-induced conformational changes of human metallothionein-2A: A combined theoretical and experimental study of metal-free and partially metalated intermediates. *J. Am. Chem. Soc. 136*, 9499−9508.

(27) Yu, X., Wu, Z., and Fenselau, C. (1995) Covalent sequestration of melphalan by metallothionein and selective alkylation of cysteines. *Biochemistry 34*, 3377−3385.

(28) Zaia, J., Jiang, L., Han, M. S., Tabb, J. R., Wu, Z., Fabris, D., and Fenselau, C. (1996) A binding site for chlorambucil on metallothionein. *Biochemistry 35*, 2830−2835.

DOI: 10.1021/acs.biochem.5b00545
Biochemistry 2015, 54, 6021−6028

(29) Chen, S.-H., Russell, W. K., and Russell, D. H. (2013) Combining chemical labeling, bottom-up and top-down ion-mobility mass spectrometry to identify metal-binding sites of partially metalated metallothionein. *Anal. Chem. 85*, 3229−3237.
(30) Apuy, J. L., Chen, X., Russell, D. H., Baldwin, T. O., and Giedroc, D. P. (2001) Ratiometric pulsed alkylation/mass spectrometry of the cysteine pairs in individual zinc fingers of MRE-binding transcription factor-1 (MTF-1) as a probe of zinc chelate stability. *Biochemistry 40*, 15164−15175.
(31) Apuy, J. L., Busenlehner, L. S., Russell, D. H., and Giedroc, D. P. (2004) Ratiometric pulsed alkylation mass spectrometry as a probe of thiolate reactivity in different metalloderivatives of Staphylococcus aureus pI258 CadC. *Biochemistry 43*, 3824−3834.
(32) Hill, B. G., Reily, C., Oh, J. Y., Johnson, M. S., and Landar, A. (2009) Methods for the determination and quantification of the reactive thiol proteome. *Free Radical Biol. Med. 47*, 675−683.
(33) Fontaine, S. D., Reid, R., Robinson, L., Ashley, G. W., and Santi, D. V. (2015) Long-term stabilization of maleimide-thiol conjugates. *Bioconjugate Chem. 26*, 145−152.
(34) Wilker, J. J., and Lippard, S. J. (1997) Alkyl transfer to metal thiolates: Kinetics, active species identification, and relevance to the DNA, methyl phosphotriester repair center of escherichia coli ada. *Inorg. Chem. 36*, 969−978.
(35) Krezel, A., and Maret, W. (2007) Different redox states of metallothionein/thionein in biological tissue. *Biochem. J. 402*, 551−558.
(36) Bernhard, W. R., Vasak, M., and Kagi, J. H. (1986) Cadmium binding and metal cluster formation in metallothionein: a differential modification study. *Biochemistry 25*, 1975−1980.
(37) Bernhard, W. R. (1991) Differential modification of metallothionein with iodoacetamide. *Methods Enzymol. 205*, 426−433.
(38) Irvine, G. W., Duncan, K. E., Gullons, M., and Stillman, M. J. (2015) Metalation kinetics of the human alpha-metallothionein 1a fragment is dependent on the fluxional structure of the apo-protein. *Chem. - Eur. J. 21*, 1269−1279.
(39) Zinnel, N. F., Pai, P.-J., and Russell, D. H. (2012) Ion mobility-mass spectrometry (IM-MS) for top-down proteomics: Increased dynamic range affords increased sequence coverage. *Anal. Chem. 84*, 3390−3397.
(40) Lobinski, R., Chassaigne, H., and Szpunar, J. (1998) Analysis for metallothioneins using coupled techniques. *Talanta 46*, 271−289.
(41) Chen, S.-H., and Russell, D. H. (2015) How Closely Related Are Conformations of Protein Ions Sampled by IM-MS to Native Solution Structures? *J. Am. Soc. Mass Spectrom. 26*, 1433−1443.
(42) Kurono, S., Kurono, T., Komori, N., Niwayama, S., and Matsumoto, H. (2006) Quantitative proteome analysis using D-labeled N-ethylmaleimide and 13C-labeled iodoacetanilide by matrix-assisted laser desorption/ionization time-of-flight mass spectrometry. *Bioorg. Med. Chem. 14*, 8197−8209.
(43) Jiang, L. J., Vasak, M., Vallee, B. L., and Maret, W. (2000) Zinc transfer potentials of the alpha - and beta-clusters of metallothionein are affected by domain interactions in the whole molecule. *Proc. Natl. Acad. Sci. U. S. A. 97*, 2503−2508.
(44) Cols, N., Romero-Isart, N., Capdevila, M., Oliva, B., Gonzàlez-Duarte, P., Gonzàlez-Duarte, R., and Atrian, S. (1997) Binding of excess cadmium(II) to Cd7-metallothionein from recombinant mouse Zn7-metallothionein 1. UV-VIS absorption and circular dichroism studies and theoretical location approach by surface accessibility analysis. *J. Inorg. Biochem. 68*, 157−166.
(45) Blindauer, C. A. (2014) Metallothioneins. In *Binding, Transport and Storage of Metal Ions in Biological Cells* (Maret, W., and Wedd, A., Eds.) pp 606−665, The Royal Society of Chemistry, Cambridge, U.K.
(46) Zangger, K., Oz, G., Otvos, J. D., and Armitage, I. M. (1999) Three-dimensional solution structure of mouse [Cd7]-metallothionein-1 by homonuclear and heteronuclear NMR spectroscopy. *Protein science: a publication of the Protein Society 8*, 2630−2638.
(47) Bernhard, W. R., Vasak, M., and Kagi, J. H. R. (1987) Cadmium binding and metal cluster formation in metallothionein: A differential modification study. In *Metallothionein II* (Bernhard, W. R., Ed.) pp 243−246, Birkhauser, Basel, Switzerland.
(48) Nielson, K. B., and Winge, D. R. (1983) Order of metal binding in metallothionein. *J. Biol. Chem. 258*, 13063−13069.
(49) Sutherland, D. E., and Stillman, M. J. (2008) Noncooperative cadmium(II) binding to human metallothionein 1a. *Biochem. Biophys. Res. Commun. 372*, 840−844.
(50) Palacios, O., Atrian, S., and Capdevila, M. (2011) Zn- and Cu-thioneins: a functional classification for metallothioneins? *JBIC, J. Biol. Inorg. Chem. 16*, 991−1009.
(51) Chiou, S. J., Riordan, C. G., and Rheingold, A. L. (2003) Synthetic modeling of zinc thiolates: quantitative assessment of hydrogen bonding in modulating sulfur alkylation rates. *Proc. Natl. Acad. Sci. U. S. A. 100*, 3695−3700.
(52) Yu, W. H., Cai, B., Gao, Y., Xie, Y., and Huang, Z. X. (2002) Expression, characterization, and reaction of recombinant monkey metallothionein-1 and its C33M mutant. *J. Protein Chem. 21*, 177−185.

DOI: 10.1021/acs.biochem.5b00545
Biochemistry 2015, 54, 6021−6028